*Chaotic Modeling and Simulation (CMSIM) 2: 143–152, 2016*

# Localized patterns of sand ripples generated by steady flows: experimental and theoretical study

Anthony Auzerais[1], Armelle Jarno[1], Alexander Ezersky[2], and François Marin[1]

[1] LOMC, UMR 6294 CNRS, University of Le Havre, Le Havre, France
(E-mail: anthony.auzerais@univ-lehavre.fr)
(E-mail: armelle.jarno-druaux@univ-lehavre.fr)
(E-mail: francois.marin@univ-lehavre.fr)
[2] M2C, UMR 6143 CNRS University of Caen, Caen, France
(E-mail: alexander.ezersky@unicaen.fr)

**Abstract.** In recent decades, the study of mechanisms of localized structures formation in non-equilibrium media attracted attention of researchers. Such structures were found in chemically active media, in granular materials, and in many numerical experiments with model equations. In this paper we investigate theoretically and experimentally localized patterns on sandy bottoms arising under the influence of steady flows in the vicinity of vertical obstacle. Present experiments performed in a hydrodynamic channel show that spatially periodic quasi-stationary patterns whose width increases downstream in the wake of an obstacle arise from a sub-critical instability of the water-sandy bottom interface. We study the dependence of the topology of the area occupied by patterns on the flow velocity. It is shown that the characteristics of pattern on the bottom can be explained using the Swift-Hohenberg equation. Experiments show that for a correct description of structures, supplemented terms which take into account the impact of the vortices arising in the wake of an obstacle must be added into the Swift-Hohenberg equation.

**Keywords:** Sand ripples, pattern formation, steady currents, vortices, Swift-Hohenberg equation.

## 1 Introduction

The interface between water flow and sand bottom is unstable to perturbations with zero phase velocity. This instability is studied in detail for over a hundred years (Dey 2014 [2]). It was found that the development of this instability may lead to the generation of different stationary patterns at the bottom: roller structures, modulated rollers, cellular structures consisting of rhombus or squares. These structures were studied in detail for the case of super critical instability when spatially periodic pattern arose from infinitesimal perturbations and occupied the area substantially greater than the period of the pattern. In

Received: 26 March 2015 / Accepted: 10 February 2016

ISSN 2241-0503

this paper, we investigate the localized patterns. These patterns appear on the sandy bottom as a result of sub critical instability under the influence of finite-amplitude perturbations. Finite amplitude perturbations can be caused by an obstacle in the flow. It should be noted that around an obstacle, under the influence of vortices in the sandy bottom there appears a deepening - a localized structure, the so-called scour (Breusers *et al.* 1977 [1], Hoffmans and Verheij 1997 [5], Niedorada 1982 [8], etc.). Features of the scour have been investigated in detail, as they are essential for the design of hydraulic structures (Qi and Gao 2014 [9], Melville and Coleman 2000 [7], Sumer and Fredsøe 2002 [10], Whitehouse 1998 [12], Ettema 2011 [3], etc.). Our research concerns sand structures appearing under the influence of vortices in the wake at some distance from the obstacle. In our experimental conditions in the absence of vortex, the boundary water - sand is stable with respect to small perturbations. Vortices contribute to finite perturbations and initiate development patterns on the sandy bottom. Such a mechanism of occurrence of localized patterns is investigated in this paper. Paper is organized as follows. First of all, we present the hydrodynamic channel where experiments are performed, followed by results we obtained. After this, we present a theoretical model and a comparison of these eperimental and theoretical results is exposed to finally conclude.

## 2 Methods and materials

The experiments were carried out in a 0.5 m wide, 10 m long flume in 0.2 cm water depth. This hydrodynamic channel is able to generate a current as illustrated in Figure 1:

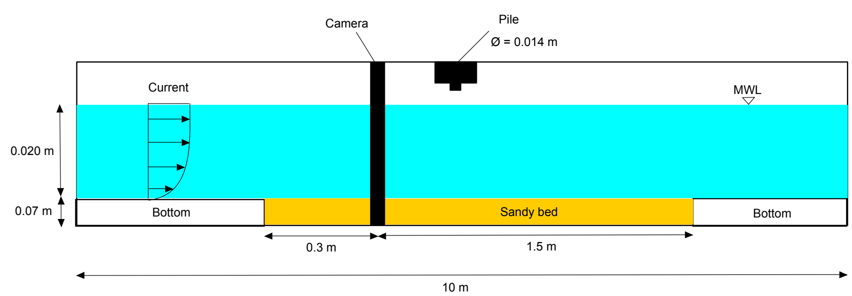


**Fig. 1.** Sketch of the experimental setup

We adopted a bed consisting of a 0.07 m sand layer where a cylindrical cylinder with diameter D=0.014m is embedded. The sediments have a relative density $s = 2.7$ and a median size $D_{50} = 340\mu m$. The experiments were performed under current without waves in subcritical regime ($\theta < \theta_c$), where $\theta$ is the Shields number:

$$\theta = \frac{\tau_0}{(\rho s - \rho).g.D_{50}} \tag{1}$$

$\tau_0$ the bed shear stress, $\rho_s$ the density of the sediment, $\rho$ the density of the fluid and $g$ the acceleration due to gravity. Shields number is a dimensionless number that represents the ratio between the forces which tend to move the sediments and those which stabilize the sediments and above a critical threshold ($\theta_c$), the live-bed regime is reached. All our experiments were carried out in the clear-water regime ($\theta < \theta_c$), thus, the sedimet transport is only due to the presence of the cylinder, generating vortices responsible of particles motion. To characterize the flow, we use the Reynolds number defined as follows:

$$Re = \frac{V.H}{\nu} \tag{2}$$

where $V$ is the mean velocity of the flow, $H$ the water depth and $\nu$ the kinematic viscosity of the fluid. To characterize regime in Karman street, another Reynolds number is used:

$$Re_d = \frac{V.d}{\nu} \tag{3}$$

with d the diameter of cylinder.

In order to estimate the pressure forces acting at the soil-water interface, we used an optical method, namely the particle image velocimetry (PIV) as shown in Figure 2, without sediment:

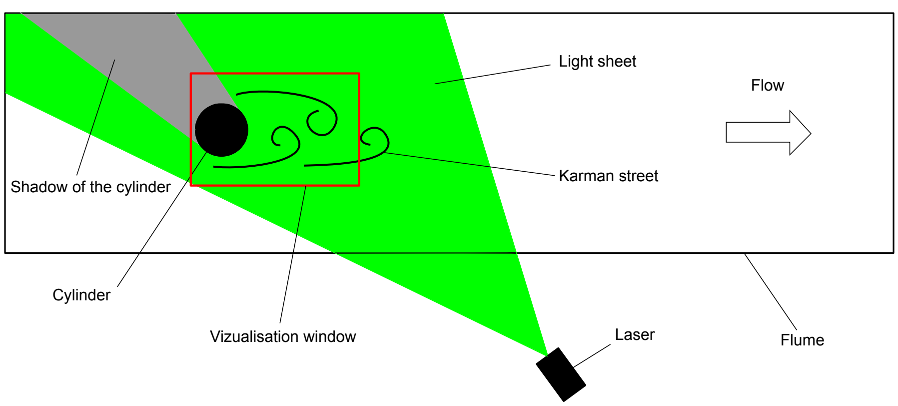


**Fig. 2.** Sketch of the PIV

This method allows to obtain the velocity field near the bottom and to deduce the hydrodynamics forces acting on the sand bed, using a horizontal laser plane. The acquisition frequency is 15 Hz, the vizualisation window side is 12 x 8 cm and the resolution of the camera is 4 Mega pixels.

## 3 Experimental results

In the experiments, we observed sediment structures formed downstream the cylinder. The experiments were performed during 50 hours at least to be sure to reach the quasi-equilibrium state of formed patterns. Patterns are shown below in Figures 3, 4 and 5 for a Reynolds number $Re$ of 38000, 42000 and 43000, respectively:

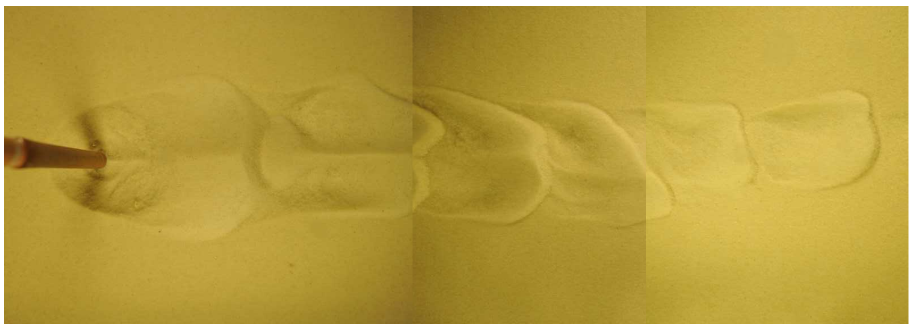

**Fig. 3.** Sedimentary structures downstream the cylinder; Re=38000 (Test 1)

**Fig. 4.** Sedimentary structures downstream the cylinder; Re=42000 (Test 2)

A significant change between the patterns is the lateral extension of sediment structures (transversal width) which is function of the velocity flow. Indeed, this lateral extension increases with the velocity flow. It can be observed that a slight variation of the Reynolds number $Re$ leads to an important difference of width for the transversal and longitudinal extension.

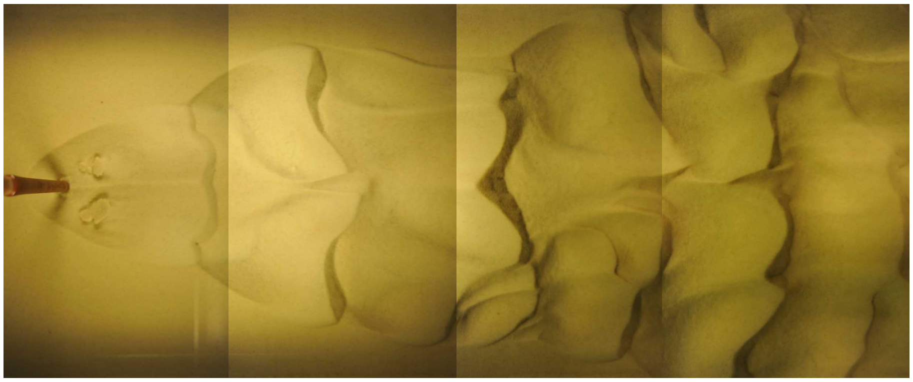

**Fig. 5.** Sedimentary structures downstream the cylinder; Re=43000 (Test 3)

Let us consider the velocity fluctuations field, shown in Figure 6 for Re= 42000:

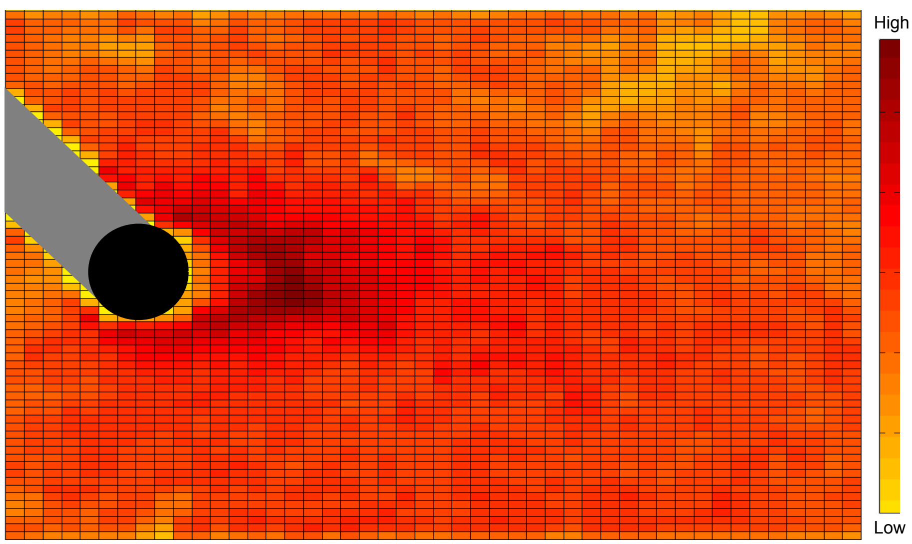


**Fig. 6.** Amplitude of velocity fluctuations in an horizontal plane 2 cm above the bed (Re=42000)

We observe that the amplitude of velocity fluctuations is very important right behind the cylinder; this amplitude decreases for increaing values of the distance to the cylinder, and increases for increasing values of $Re_d$. However, the size of the area with a high amplitude is the same regardless the value of $Re_d$.

## 4 Theoretical model

In order to modelize the observed patterns, we use the Swift-Hohenberg equation (Swift and Hohenberg [11]), a phenomenological equation:

$$\frac{\partial u}{\partial t} = \varepsilon u - (1 + \nabla^2)^2 u + qu^2 - u^3 \tag{4}$$

where:

$$\boldsymbol{\nabla} = \overrightarrow{x_0}\frac{\partial}{\partial x} + \overrightarrow{y_0}\frac{\partial}{\partial y} \tag{5}$$

$\varepsilon$ corresponds to the linear instability of the system. In this equation, instability to infinitesimal perturbations occurs if $\varepsilon > 0$. If $\varepsilon < 0$, linear instability is absent. $q$ corresponds to quadratic instability.

Swift-Hohenberg equation is widely used to describe pattern formation (Lloyd and Sandstede [6], Hilali *et al.* [4], etc.). With a flow in one direction, this equation becomes:

$$\frac{\partial u}{\partial t} = \varepsilon u - \left(1 + \frac{\partial^2}{\partial x^2}\right)^2 u + \frac{\partial^2}{\partial y^2} + qu^2 - u^3 \tag{6}$$

In our case, $\varepsilon < 0$ because our experiments were carried out in subcritical regime ($\theta < \theta_c$), therefore patterns forms only in the wake of the cylinder where velocity and pressure perturbations are important.

This equation can be modified as follows:

$$\frac{\partial u}{\partial t} = -Eu - \left(1 + \frac{\partial^2}{\partial x^2}\right)^2 u + \frac{\partial^2}{\partial y^2} + qu^2 - u^3 + f(x, y, t) \tag{7}$$

$E$ is proportional to $V - V_c$ where $V$ is velocity of flow in our experiments. It means that if $V > Vc$ ($V_c$ is critical velocity), $E < 0$ instability occurs everywhere, and if $V < Vc$, $E > 0$ instability occurs in the wake of the cylinder, where perturbations with final amplitudes exist. We take into account the influence of these perturbations adding force f(x,y,t) into Swift-Hohenberg equation. We suppose that this force is proportional to $V^2$, where $V^2$ is spatially modulated random field, because for Reynolds numbers $Re_d$ of several thousand in our experiment turbulent Karman street is observed. Amplitude of velocity fluctuations is approximated using experimental data presented in Figure 6. The shape of this force can be qualitatively explained as follows.

According to Bernoulli's equation, we can write along a streamline:

$$P + \rho\frac{V^2}{2} = constant \qquad (=) \qquad P = constant - \rho\frac{V^2}{2} \tag{8}$$

a decrease of pressure inducing an increase of velocity, low pressure corresponds to positive forces acting at the sand-water interface. This force introduces perturbations on water-sand bottom interface.

## 5 Comparison theory-experiments

The theoretical model allows to reproduce qualitatively the patterns observed experimentally, test parameters are listed in Table 1. Figures 7,8 and 9 show the superposition of theoretical and experimental results. At the bottom of Figure 7, the perturbation (due to the cylinder) resulting in patterns formation has a limited size, in particular with a weak lateral extension of sediments downstream the cylinder. The corresponding theoretical result at the top of Figure 7 displays patterns which are qualitatively in good agreement with those observed for present experiments.

| Experimental tests | | | | Theoretical tests | | | |
|---|---|---|---|---|---|---|---|
| Test number | 1 | 2 | 3 | Test number | 1 | 2 | 3 |
| Test duration (h) | 70 | 68 | 65 | Integrations numbers | 30 | 30 | 30 |
| $Re$ | 38000 | 42000 | 43000 | E | 0.23 | 0.14 | 0.07 |
| $Re_d$ | 2660 | 2940 | 3010 | q | 1.6 | 1.6 | 1.6 |

**Table 1.** Tests parameters

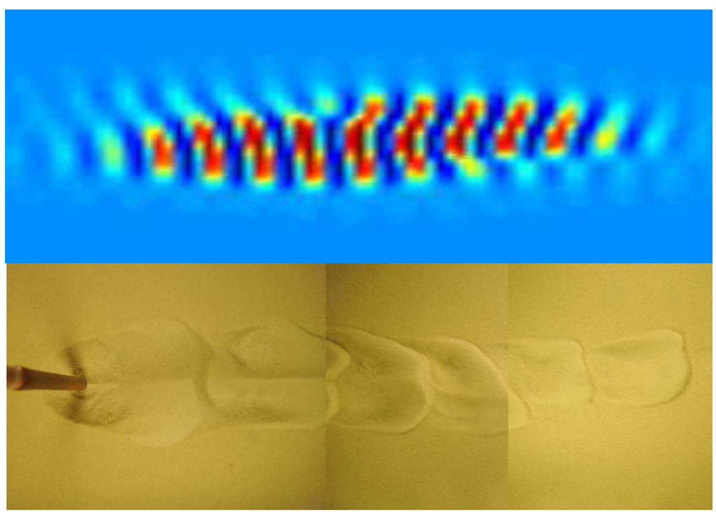

**Fig. 7.** Top: theory; Bottom: experiment (Test 1)

As far as the other tests are concerned, Figures 8 and 9 show that the pattern width increases for increasing values of the Reynolds number $Re$. This leads to a decrease of the value of the parameter $E$ in the Swift-Hohenberg equation to obtain a similar description of experimentals patterns. Thereby, the patterns simulated with the present theoretical model are consistent with our experimental results.

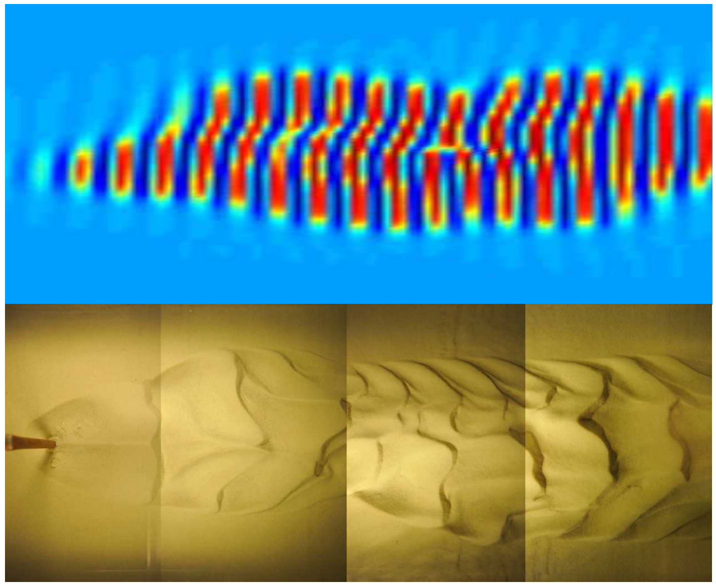

**Fig. 8.** Top: theory; Bottom: experiment (Test 2)

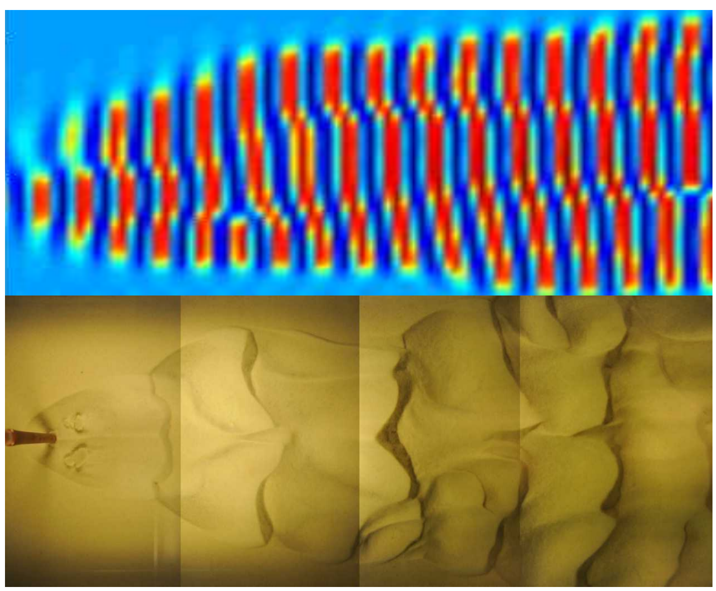

**Fig. 9.** Top: theory; Bottom: experiment (Test 3)

## Conclusions

In this paper, we investigate theoretically and experimentally localized patterns on sandy bottoms arising under the influence of steady flows downstream of a vertical obstacle simulating a pile. Experiments carried out in a hydrodynamic channel show that spatially periodic quasi-stationary patterns whose width increases downstream in the wake of a vertical cylinder arise from a sub-critical instability of the water-sandy bottom interface. The width of these spatially periodic quasi-stationary patterns increases for increasing values of the flow velocity. It is shown that the characteristics of patterns on the bottom can be explained using the Swift-Hohenberg equation. Experiments show that for a correct description of sand structures, the variation of the parameter corresponding to linear instability is sufficient.

## Acknowledgments

The authors express their sincere thanks to the High Normandy region (Scale Research Network) for funding this work.

# References


[1] Nicollett G. Shen H. Breusers, H. Local scour around cylindrical piers. *J. Hydraul. Res.*, 15:211–252, 1977.

[2] S. Dey. *Fluvial Hydrodynamics: Sediment Transport and Scour Phenomena*. Springer, 2014.

[3] Constantinescu G. Melville B. Ettema, R. *Evaluation of Bridge Scour Research: Pier Scour Processes and Predictions*. Washington, DC, 2011.

[4] Métens S. Borckmans P. Dewel G. Hilali, M'F. Localized hexagon patterns of the planar swiftâĂŞhohenberg equation. *Physical review E*, 51(3):2046–2052, March 1995.

[5] Verheij H.J. Hoffmans, G.J.C.M. *Scour Manual*. Rotterdam, Netherlands, 1997.

[6] Sandstede B. Lloyd, D. J. B. Localized hexagon patterns of the planar swiftâĂŞhohenberg equation. *J. Appl. Dynam. Syst.*, (7):1049–1100, June 2008.

[7] Coleman S.E. Melville, B.W. *Bridge Scour*. LLC, CO, USA, 2000.

[8] Dalton C. Niedorada, A. W. A review of the fluid mechanics of ocean scour. *Ocean Engng*, 9(2):159–170, 1982.

[9] Gao F. Qi, W. Equilibrium scour depth at offshore monopile foundation in combined waves and current. *Sci China Tech Sci*, 57(5):1030–1039, May 2014.

[10] Fredsøe J. Sumer, B.M. *The Mechanics of Scour in the Marine Environment*. Singapore, 2002.

[11] Hohenberg P.C. Swift, J. Hydrodynamic fluctuations at the convective instability. *Physical Review A*, 15(1):319–328, January 1977.

[12] R. Whitehouse. *Scour at Marine Structures: a Manual for Practical Applications*. London, 1998.